JOURNAL OF MATERIALS SCIENCE 28 (1993) 2738–2744

Characterization of fluorine-doped silica glasses

M. KYOTO, Y. OHOGA, S. ISHIKAWA, Y. ISHIGURO
Research and Development Group, Sumitomo Electric Industries Ltd, 1 Taya-cho, Sakae-ku, Yokohama, 244, Japan

Fluorine-doped silica glasses containing up to 2 wt% were prepared by the vapour-phase-axial-deposition (VAD) sintering process. The characteristics of these glasses were investigated by Raman spectroscopy, vacuum-ultraviolet–ultraviolet (v.u.v–u.v.) spectroscopy, and viscosity measurements. From the Raman spectroscopic investigation, it has been shown that the Si–F bond structure in the fibres is the same as that in bulk glass and is not affected by codoped additives such as B_2O_3. From the u.v.–v.u.v. spectroscopic investigation, it has been shown that the absorption band at 7.6 eV in high-purity silica glass is removed with the addition of fluorine. This addition produces a silica glass with most excellent transparency in u.v. and v.u.v. regions. Also it was observed that the optimum addition is around 1 wt%. This fact proves that fluorine incorporation in glass prevents the generation of defects related to optical loss in fibres. From the viscosity study, it was found that the viscosity decreases with an increase of the fluorine content in glass and the activation energy also decreases with increasing fluorine content.

1. Introduction

The most important dopant for preparing a pure-silica-core fibre is fluorine because this dopant depresses the refractive index of the cladding glass without any additional loss, as occurs with boron dopants [1]. Fluorine doping has been demonstrated for fibre fabrication processes by modified chemical vapour deposition (MCVD) [2, 3], and plasma chemical vapour deposition (PCVD) [4], the vapour-phase axial deposition (VAD) [5] and outside vapour-phase deposition (OVD) [6] methods.

For applications of fluorine-doped silica glass as a cladding material for pure silica fibre, its optical properties are important. Dumas *et al.* [7] reported a Raman band at 945 cm^{-1} due to Si–F bonds and suggested that a [$SiFO_3$] tetrahedral structure existed in fluorine-doped glass. Rabinovich [8] suggested that the refractive-index reduction in glass was caused by this structure, which was formed by a substitution reaction of oxygen with fluorine. He also pointed out that this substitution decreased the non-bridging oxygen defects, which are closely related to optical losses in glass.

Recently, however, several studies of fluorine-doped silica glasses have suggested a structural change of the Si–F bond and revealed some kinds of optical loss closely related to the defects caused by fluorine incorporation in silica glass [9, 10]. For instance, Noguchi *et al.* [11] reported a slight difference between the wave numbers of the Si–F bond in bulk and fibre glasses. They suggested that this difference was caused by the internal stress applied to the fibre core or by the internal changes due to the other dopants. Imai *et al.* [12] reported that three new Raman bands were observed at around 1050–1100, 880 and 980 cm^{-1} in fluorine-doped silica glass prepared at a high temperature (1750 °C). They suggested that the first band is due to the non-bridging-oxygen-centre defects and the last two are due to a different form from SiO_3F. Hibino *et al.* [13] studied the optical loss in the fluorine-doped fibres and found that the loss was induced by the process of drawing the fibre. Yonemori *et al.* [14] suggested from an NMR study that the fluorine is probably bonded to the boron in fluorine and boron codoped glasses. These findings suggested that the optical properties of fluorine-doped glass should be closely related to fabrication parameters, such as the preparation method, purification and stoichiometric controls, and drawing conditions. From this standpoint, there is still a lack of understanding of the material characteristics of fluorine-doped silica glasses. Therefore, further investigation of the characteristics of the fluorine-doped silica glass is essential.

In this paper, we have investigated the characteristics of a fluorine-doped glass prepared by the VAD sintering process by using Raman spectroscopy, v.u.v.–u.v. spectroscopy, and viscosity measurement.

2. Experimental procedure

2.1. Sample preparation

Bulk and fibre glass samples were prepared using the VAD fibre fabrication method. All soot samples, which were intermediate products, were dehydrated and purified by chlorine treatment and then consolidated into the glass samples. The details were as follows.

Porous preforms were synthesized by a single torch as shown schematically in Fig. 1a. Raw material, $SiCl_4$ was fed into the torch. In the oxyhydrogen flame, fine soot particles were synthesized and the particles were

0022–2461

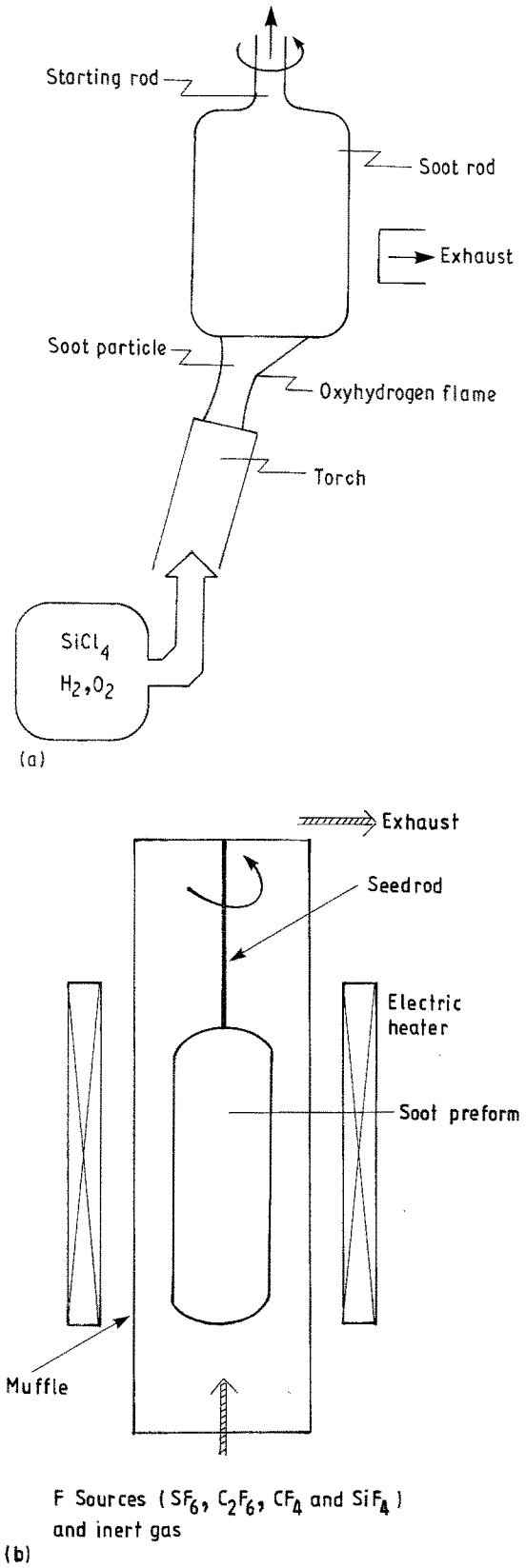

Figure 1 (a) Schematic diagram of the experimental soot deposition. (b) Schematic diagram of the fluorine doping in sintering process for basic investigation.

deposited on the end surface of a starting rod which was rotated while being pulled upwards at the same speed as the soot-deposition growth rate. The porous soot was dehydrated in a chlorine treatment and next heated in a stream of fluorine and helium gas in an electric furnace at a given temperature as shown schematically in Fig. 1b. Finally, the soot was consolidated to a transparent glass preform. The glass preform was elongated and jacketed with a pure-silica tube, which was used as the reference for refractive-index measurement. The refractive indexes of the resulting glasses were measured using a preform analyser.

2.2. Raman spectroscopic analysis

Raman spectra were measured using a Raman spectrometer with a double monochrometer. The excitation wavelength was 4880 nm from an ionized argon laser (JASCO NR1100). The Raman spectra of bulk glasses were measured at an angle about 90° to the incident laser beam. For the fibre samples, a microfocused laser beam was directly inserted into one end of the fibre and transmitted through the fibre. The light emitted from the other end of the fibre was analysed using the Raman spectrometer. The input power was 0.1 W and fibre was 5–1000 m in length.

2.3. U.v. and v.u.v. spectroscopic analysis

V.u.v. (vacuum ultraviolet) absorption spectra from 120 nm to 260 nm were measured in a low-pressure atmosphere using a single-beam spectrometer monochrometer (JASCO v.u.v.-200) as shown in Fig. 2. The light source was a D_2 lamp, and the intensity of transmitted light was detected by a photomultiplier. Glass samples were cut and polished into plates having an optical path of 1 mm. U.v. absorption spectra from 190 to 500 nm were measured using a double-beam spectrometer (HITACHI U-3400).

2.4. Viscosity measurements

Viscosity was measured by the conventional penetration method [15]. The viscosity of the glass samples were observed at temperatures of 1080, 1180 and 1280 °C. Glass samples were cut and polished into plates 30 mm in diameter and 5 mm thick.

3. Results and discussion

3.1. Raman spectroscopic analysis

3.1.1. Drawing effect on the Si–F bonds

Fig. 3 shows a typical Raman spectra of SiO_2, F–SiO_2 bulk glasses in the wavelength region 50–1500 cm^{-1}. The spectrum of SiO_2 shows peaks at 440 (Si–O rocking vibration), 805 (stretching vibration) and at 1065 and 1200 cm^{-1} (stretching vibrations). The sharp

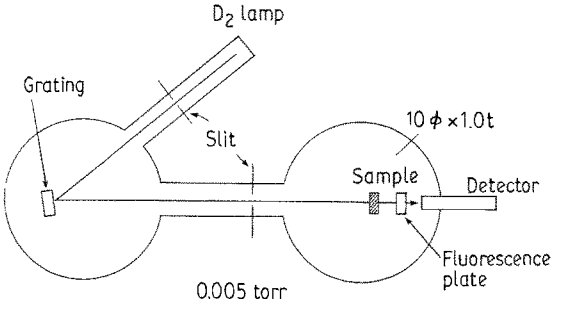

Figure 2 Apparatus of absorption measurements in v.u.v. region.

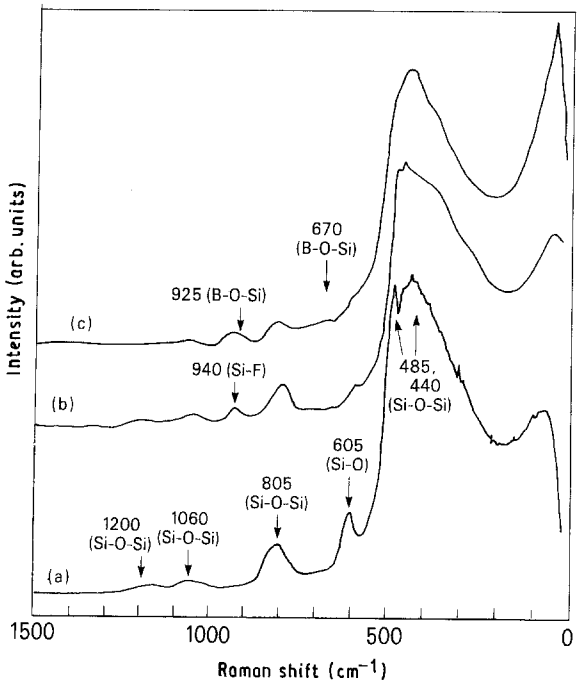

Figure 3 Typical Raman spectra of SiO_2, F–SiO_2 and B_2O_3–SiO_2 glasses (a) SiO_2; (b) F–SiO_2; $\Delta n = -0.75\%$; (c) B_2O_3–SiO_2; $\Delta n = -0.40\%$.

peaks at 485 and 605 cm^{-1} were assigned to four-membered and three-membered rings of Si–O bonds [16], by which the structural strain on the bonds is caused. In the spectra of the F–SiO_2 glass, an additional peak was observed at 945 cm^{-1} and assigned to the Si–F stretching bond of a [SiO_3F] tetrahedron. The intensity of the bands at 485 and 605 cm^{-1} decreases with fluorine doping [17].

Fig. 4 shows the Raman spectra, bulk and fibre, of F–SiO_2. In the spectra of fibre, the peak due to the Si–F band is observed at 940 cm^{-1} as in the spectra of bulk glass. This fact shows that the Si–F bond is not affected by the internal stress applied to the fibre.

Fig. 5 shows the intensity of the peak at 940 cm^{-1} relative to that at 805 cm^{-1} as a function of the relative refractive-index difference, Δn, which is proportional to the fluorine content in F–SiO_2 glass. The intensity increases linearly with fluorine content even in fibre, thus confirming that the Si–F bond in fibre is the same as that in bulk glass. This fact supports the theory that the [SiO_3F] tetrahedron structure maintains chemical stability during the fibre drawing process, in which high temperature and strong stress are applied to the fibre.

3.1.2. Codoping effect on fluorine

Fig. 6 shows the typical Raman spectra of B_2O_3–SiO_2 and F–B_2O_3–SiO_2 glasses. These glasses were prepared by using BCl_3 and BF_3 gases as the starting material to lower the refractive index, the relative refractive-index differences were -0.3% and -1%, respectively. In the spectra of B_2O_3–SiO_2 glass, a characteristic peak at 925 cm^{-1} was observed. Shibata *et al.* [18] showed that this peak could be ascribed to the B–O–Si bond; and the intensity increases linearly with the B_2O_3 content in the glass.

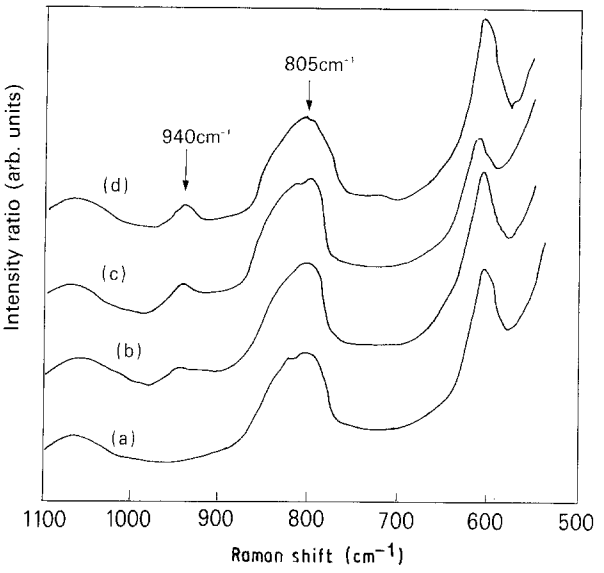

Figure 4 Raman spectra of F–SiO_2 glasses. (a) SiO_2 (bulk), (b) $\Delta n = -0.20\%$ (fibre), (c) $\Delta n = -0.30\%$ (bulk), (d) $\Delta n = -0.45\%$ (fibre).

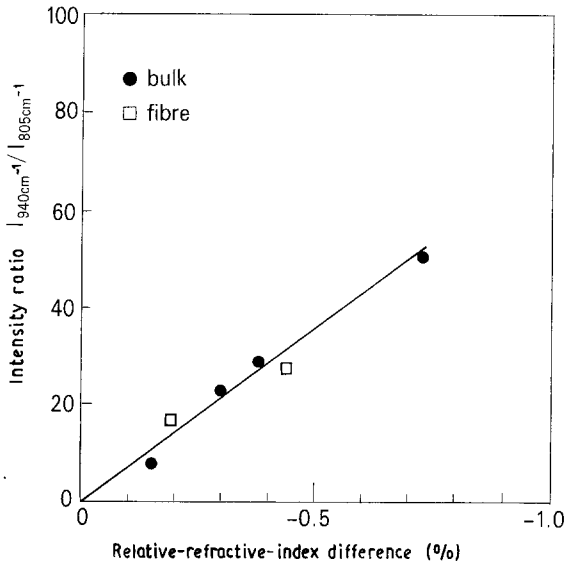

Figure 5 Relationship between relative refractive index difference and the intensity ratio of $I_{940\,cm^{-1}}/I_{805\,cm^{-1}}$ in bulk and fibre.

This linearity was also obtained in the present work, as shown in Fig. 7. In the spectra of F–B_2O_3–SiO_2 glass as shown in Fig. 8, a characteristic peak appears only at 940 cm^{-1} but the shape is slightly broader and a little asymmetric compared with that of Si–F bond peaks. This asymmetry suggests an overlap of the two peaks due to Si–F and B–O–Si bonds.

This asymmetric peak was resolved into two peaks with a Gaussian shape by using the Gaussian-decomposition method; these peaks appeared at 942 and 922 cm^{-1}, as shown in Fig. 8. If the peaks are attributed to Si–F and B–O–Si bonds, the contributed values are estimated to be -0.7% for Si–F and -0.3% for B–O–Si. Their sum is the same as the total Δn (-1.0%) measured by a preform analyser. The lowering in the refractive index of F–B_2O_3–SiO_2 has a contribution from the Si–F and B–O–Si bonds. It is clear that fluorine atoms preferentially bond with

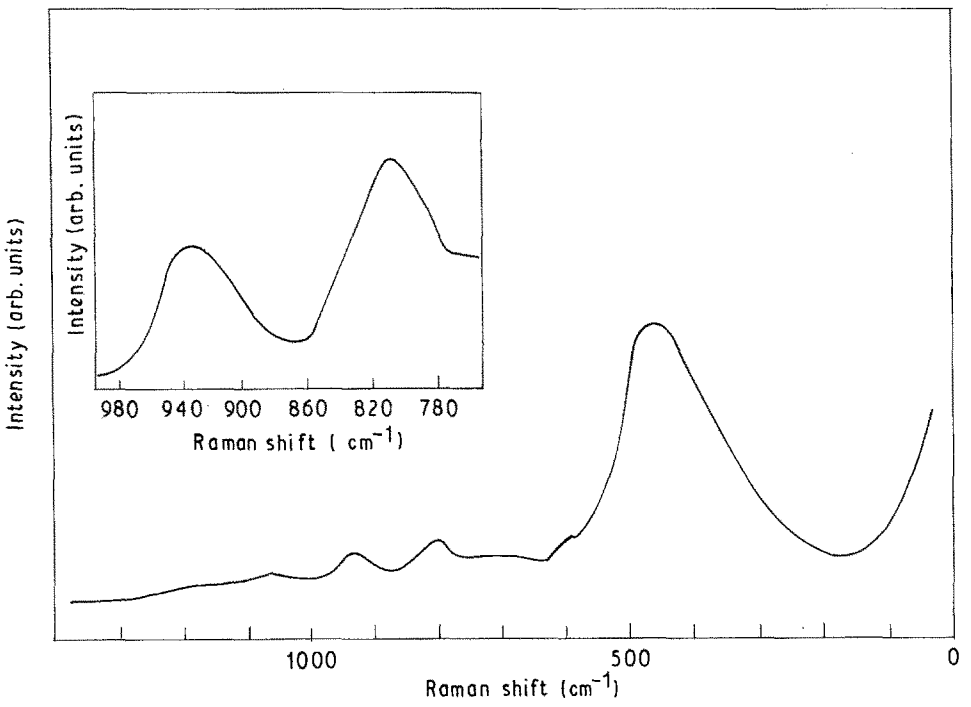

Figure 6 Raman spectra of F–B_2O_3–SiO_2 glass, $\Delta n = -1.0\%$

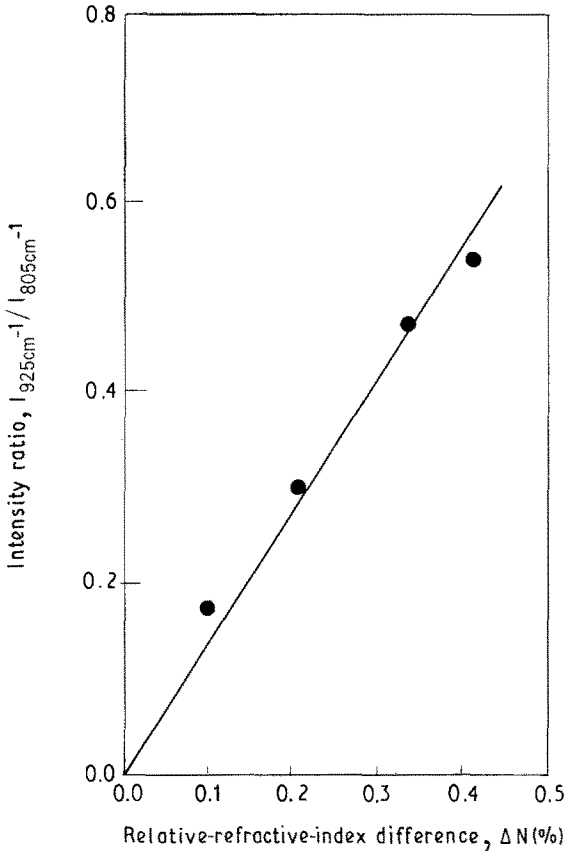

Figure 7 Relationship between relative refractive index diference and the intensity ratio of $I_{925\,cm^{-1}}/I_{805\,cm^{-1}}$.

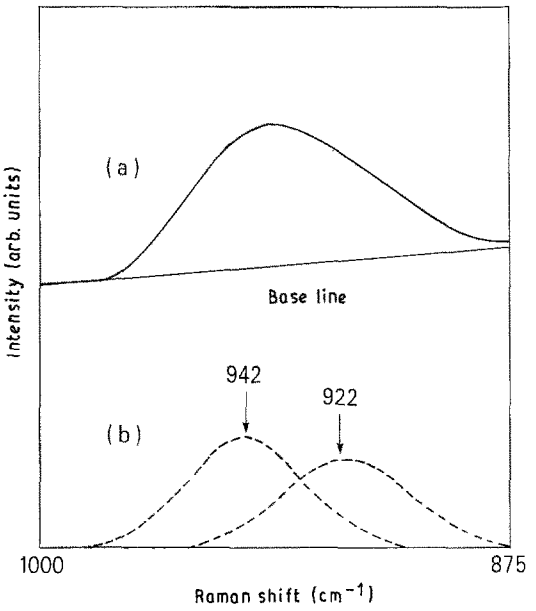

Figure 8 Raman actual peak and its separated peaks by using gaussion decomposition.

TABLE I Preparation of glass samples by VAD

Sample name	Process
A Pure SiO_2	Dehydration by chlorine
B Pure SiO_2 glass (H_2 treatment)	Heat treatment with a H_2 atmosphere at 700 °C for 5 h
C GeO_2–SiO_2	Doping of GeO_2 in soot deposition
D F–SiO_2	Incorporation of fluorine in sintering

Si and form a [SiO_3F] tetrahedron even under B_2O_3 codoping.

3.2. U.v. and v.u.v. spectroscopic analysis

Four types of glass sample were prepared by using the VAD method, as shown in Table I. Samples A and B were pure-silica glasses; sample A was dehydrated by using chlorine gas and sample B was immersed in hydrogen at 700 °C for 5 h followed by dehydration. Sample C was a silica glass codoped with a small amount of GeO_2 during the VAD soot-deposition

process and dehydrated. Sample D was a silica glass doped with fluorine during the consolidation process.

Fig. 9 shows the v.u.v. spectra of the dehydrated silica glass. An absorption peak appears at 7.6 eV, which is assigned to the oxygen-deficient centre ≡Si:Si≡ (where ≡ indicates three separate bonds to oxygen) [19]. The 7.6 eV peak intensity increases with an increase of chlorine content in the glass. This fact suggests that the Si:Si defects are generated by the following condensation reaction Si–Cl bonds during the sintering process.

$$\equiv Si{-}Cl + Cl{-}Si\equiv \rightarrow Si{:}Si\equiv + Cl_2 \quad (1)$$

Fig. 10 shows the v.u.v. spectra of F–SiO_2, GeO_2–SiO_2 and pure SiO_2, before and after annealing in a hydrogen atmosphere. The peak at 7.6 eV in pure SiO_2 was dramatically reduced after hydrogen annealing and this peak disappeared in the F–SiO_2 and GeO_2–SiO_2 glasses. Furthermore, the rapid increase in absorption of F–SiO_2 shifted toward wavelengths shorter than that of pure SiO_2. These phenomena suggest that the Si:Si bonds are decomposed by additives such as hydrogen, GeO_2 and fluorine during Reactions (2–4), respectively.

Hydrogen annealing reaction

$$\equiv Si{:}Si\equiv + H_2 \rightarrow 2\equiv Si{-}H \quad (2)$$

Oxidation reaction by GeO_2

$$GeO_2 \rightarrow GeO + \tfrac{1}{2}O_2$$

$$\equiv Si{:}Si\equiv + \tfrac{1}{2}O_2 \rightarrow \equiv Si{-}O{-}Si\equiv \quad (3)$$

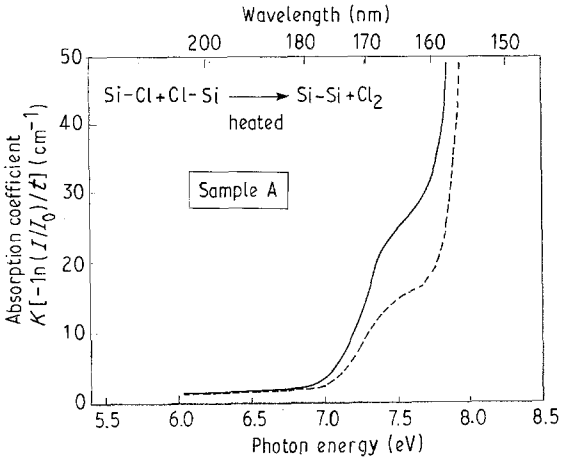

Figure 9 Effect of chlorine on the absorption in v.u.v. region.

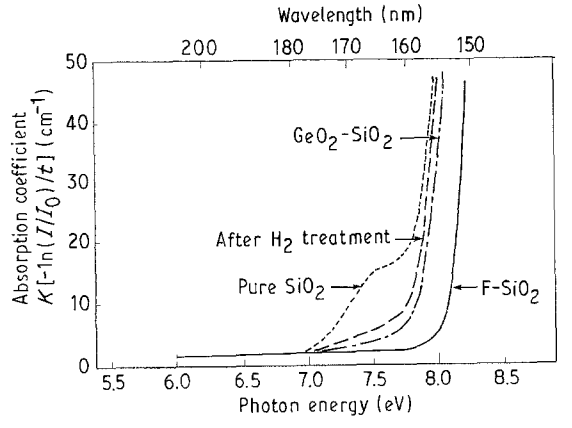

Figure 10 Effect of additives on the absorption in v.u.v. region.

Fluoridation reaction

$$\equiv Si{:}Si\equiv + 2F \rightarrow 2\equiv Si{-}F$$

$$\equiv Si{-}Cl + F \rightarrow \equiv Si{-}F + Cl \quad (4)$$

In the case of fluorine addition, the substitution reaction of Cl for F, Reaction (4), should also occur during the consolidation process because the combined energy of the Si–F bond is larger than that of the Si–Cl bonds. In other words, the precursor, Si–Cl, of the Si:Si defect disappears in F–SiO_2 glass.

Fig. 11 shows the optical absorption u.v. spectra of various glasses. The dehydrated glass has a large peak at 5.0 eV caused by oxygen-vacancy defects. This 5.0 eV band was also reduced during the hydrogen annealing at 700 °C. The addition of GeO_2 in silica glass suppressed the 7.6 eV defect absorption, but this addition caused the strong absorption, which is closely related to GeO generation.

Fig. 12 shows the v.u.v. spectra of pure SiO_2 and F–SiO_2 glasses with fluorine compositions of 1 and 2 wt %. The spectra show that the rapid increase of v.u.v. absorption is shorter in F–SiO_2 glasses than in pure SiO_2 glass, and the best transparency exists at a fluorine content of around 1 wt % and not of 2 wt %.

Fig. 13 shows the spectra of F–SiO_2 glass before and after ArF (7.6 eV) excimer laser irradiation. The irradiation conditions were as follows: the power per pulse was 500 mJ cm^{-2}, and there were 5×10^5 pulses

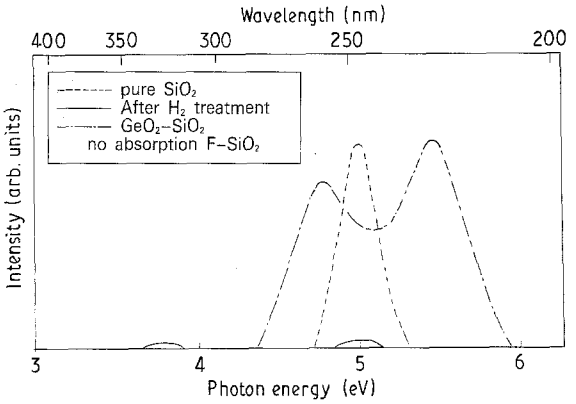

Figure 11 Optical absorption spectra of various glasses in u.v. region.

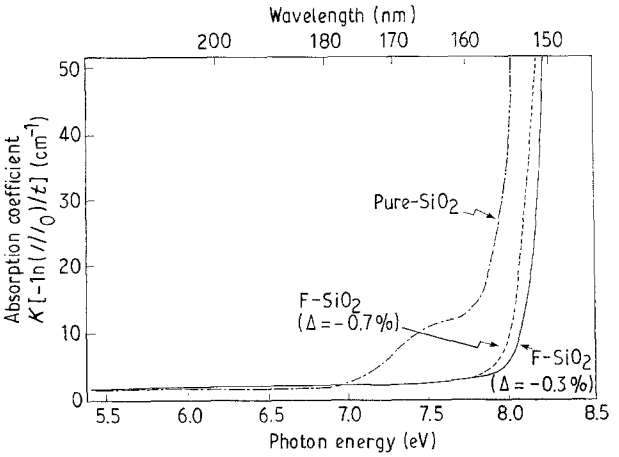

Figure 12 Absorption characteristics of SiO_2, F–SiO_2 ($\Delta n = -0.3\%$ and F–SiO_2 ($\Delta n = -0.7\%$) in v.u.v. region.

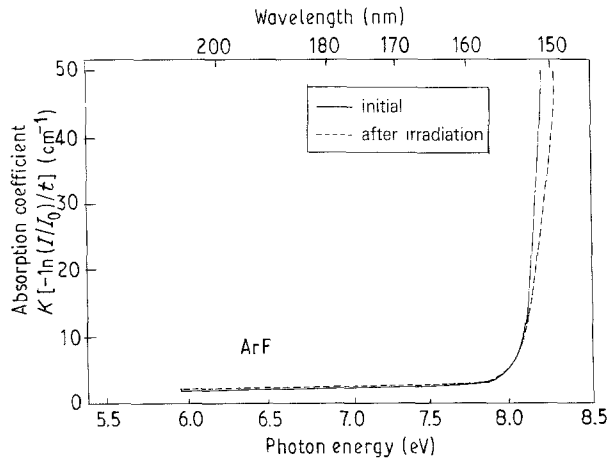

Figure 13 Absorption characteristics of F–SiO_2 irradiated by ArF (6.4 ev) excimer laser (500 J/cm^2. Pulse × 5 × 10^5 pulse.

in total, and the frequency was 60 Hz. The solid and dotted lines show the spectra before and after irradiation respectively. There is no change before or after irradiation in optical absorption ranging from 6.0 to 8.0 eV.

In conclusion, it is found that ≡Si:Si≡ defects in silica glass can be perfectly removed during fluorine incorporation and the best u.v.–v.u.v. transparency occurs in F–SiO_2 glass with 1 wt % fluorine content. Furthermore, this high transparency is maintained even under high-energy irradiation such as by an ArF excimer laser (6.4 eV).

3.3. Viscosity

Table II shows the viscosity data of various fluorine-content glasses. The viscosity data are plotted as a function of reciprocal temperatures, T^{-1}, as shown in Fig. 14. For fluorine content ranging from 1 wt % to 3 wt %, the viscosity obeys the Arrhenius form and decreases proportionally with the increase of fluorine content in the glass.

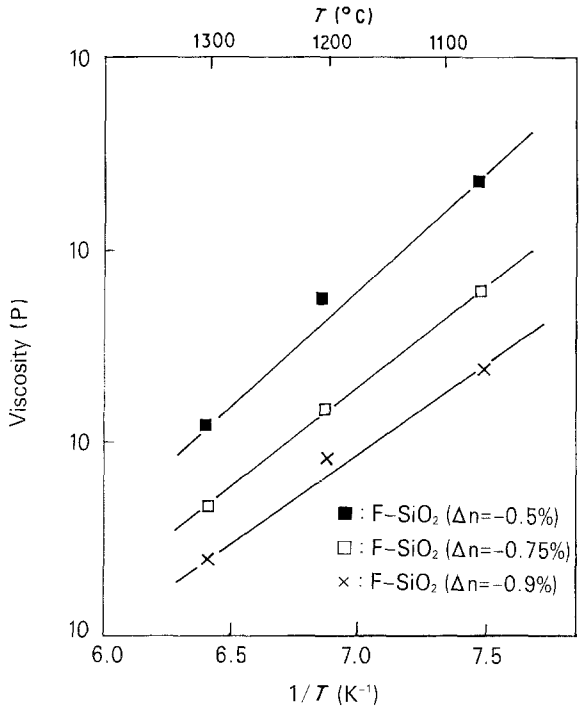

Figure 14 Arrhenius form of viscosity of F–SiO_2.

TABLE II Viscosity data of fluorine glasses

	Viscosity (P)		
Δn (%)	1080 °C	1180 °C	1280 °C
0.5	3.0×10^{10}	6.9×10^{9}	1.2×10^{9}
0.75	8.4×10^{9}	2.0×10^{9}	5.5×10^{8}
0.90	3.4×10^{9}	1.1×10^{9}	3.3×10^{8}

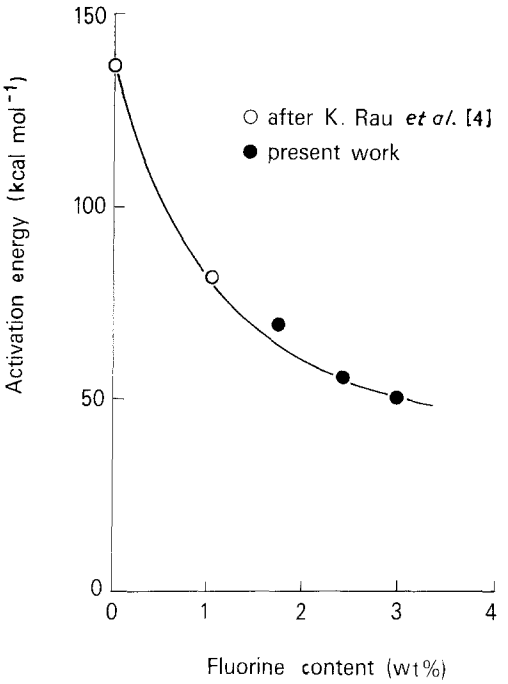

Figure 15 Activation energy of viscosity as a function of fluorine content.

Fig. 15 shows the activation energies of viscosity in these glasses as a function of fluorine content. Previously published data [4] are also plotted. Activation energy decreases with increasing fluorine content in glass. This trend strongly suggests that the viscosity decrease is caused by a weakening of [SiO_4] glass network due to the oxygen–fluorine substitution reaction in the Si–O network.

4. Conclusion

We have investigated the characteristics of fluorine-doped glass by using Raman spectroscopy, v.u.v.–u.v. spectroscopy, and viscosity measurements.

From the Raman spectroscopic investigation, the Si–F bond structure in fibre is the same as that in bulk glass and is not affected by codoped additives such as B_2O_3.

From the u.v.–v.u.v. spectroscopic investigation, it was shown that the absorption band at 7.6 eV in high-purity silica glass is removed with the addition of fluorine. This addition produces a silica glass with most excellent transparency in u.v. and v.u.v. regions. Also it was observed that the optimum addition is around 1 wt %. This fact proves that fluorine incor-

poration in glass prevents the generation of defects related to optical loss in fibre.

From the viscosity study, it is clear that the viscosity decreases with an increase of fluorine content.

In summary, the fluorine-doped silica glass prepared by the VAD sintering method has excellent features for fibre fabrication.

Acknowledgement

The authors wish to thank S. Shiomoto for the viscosity measurement.

References

1. S. SHIRAISHI, K. FUJIWARA and S. KUROSAKI, US Patent 4 082 420.
2. K. ABE, Technical digest, Second European conference on optical communication, Paris, 1976 (Comite du Colloque International sur les Transmissions par fibers (Optique, Paris, 1977) p. 59.
3. A. KAWANA, T. MIYA, S. ARAKI and Y. FURUI, *Trans. IECEJ* E65, **9** (1982).
4. K. RAU, A. MUHLICH and M. TREBER, Technical digest. Topical meeting of optical fiber transmission II, Williumsberg, 1977 (Optical Society of America, Washington).
5. M. KYOTO, H. KANAMORI, N. YOSHIOKA, G. TANAKA and M. WATANABE, Technical digest, Conference on optical fiber communication, New Orleans, LA, 1984, Paper MG5. (Optical Society of America, Washington).
6. G. E. BERKEY, *ibid.*, Paper MG3.
7. P. DUMAS, J. CORSET, W. CARVALHO, Y. LEVY and Y. NEUMAN, *J. Non-Crys. Solids* **47** (2) (1982) 239.
8. E. M. RABINOVICH, *Phys. Chem. Glasses* **24** (2) (1983) 54.
9. W. HEITMANN, H. U. BONEWITZ and A. MUHLICH, *Elec. Lett.* **19** (16) (1983) 616.
10. P. BACHMANN, P. GEITTNER, D. LEERS, M. LENNERTZ and H. WILSON, *Elec. Lett.* **20** (1) (1984) 35.
11. K. NOGUCHI, M. MURAKAMI, Y. UESUGI and K. ISHIHARA, *Appl. Phys. Lett.* **44** (5) (1984) 491.
12. H. IMAI, K. ARAI, Y. FUJIMOTO, Y. ISHII and H. NAMIKAWA, *Phys. Chem. Glasses* **29** (2) (1988) 54.
13. Y. HIBINO, H. HANAFUSA, K. EMA and S. HYODO, *Appl. Phys. Lett.* **47** (1982) 812.
14. S. YONEMORI, A. MASUI and M. NOSHIRO, *Yogyo-Kyokai-Shi* **94** (8) (1986) 863.
15. R. W. DOUGLASS, W. L. ARMSTRONG, J. P. EDWARD and D. HALL, *Glass Tech.* **6** (1965) 52.
16. F. L. GAREENER, *J. Non-Crys. Solids* **49** (1982) 53.
17. C. A. M. MULDER, R. K. JANSSEN, P. BACHMANN and D. LEERS, *J. Non-Crys. Solids* **72** (1985) 243.
18. N. SHIBATA, M. HORIGUCHI and T. EDAHIRO, *J. Non-Crys. Solids* **45** (1981) 115.
19. H. IMAI, K. ARAI, H. IMAGAWA, H. HOSONO and Y. ABE, *Phys. Rev.* **B38** (1988) 12772.

Received 12 December 1991
and accepted 25 September 1992